

# A classification of phase diagrams of ternary fluid systems†

Martin Bluma<sup>a</sup> and Ulrich K. Deiters<sup>\*b</sup>

<sup>a</sup> IBM Germany, Gustav-Heinemann-Ufer 120-122, 50968 Köln, Germany

<sup>b</sup> Institute of Physical Chemistry, University at Cologne, Luxemburger Str. 116, 50939 Köln, Germany

Received 18th June 1999, Accepted 9th August 1999

Phase diagrams and critical states of ternary fluids mixtures are calculated from the van der Waals equation of state with standard 1-fluid mixing rules. Berthelot–Lorentz combining rules are assumed for the binary interaction parameters. The topological classes of the resulting ternary phase diagrams are determined and their relationship to the classes of the binary subsystems discussed. It is shown that the phenomena of “miscibility windows” and “miscibility islands” are connected with a special ternary phase diagram class and can be reproduced even with the van der Waals equation of state.

## 1 Introduction

Since the pioneering work of van Konynenburg and Scott in 1968<sup>1</sup> on the global phase behaviour of binary fluid mixtures, based on the van der Waals equation of state, several investigations of the global phase behaviour of binary fluid mixtures were published for more complex equations of state.<sup>2–12</sup> The calculated global phase diagrams for these equations show a remarkable similarity: The same main phase diagram classes are found, and also the arrangement of their domains in the global phase diagrams are quite similar. Differences and model-specific features appear only in small sections of the global phase diagrams. Even so, a large number of phase diagram classes has been discovered until now, mostly in theory, but also the number of classes confirmed by experiment exceeds the original number, 5, by far. A rational nomenclature system for the phase diagram classes, which thus became necessary, has been proposed elsewhere.<sup>13</sup>

No equivalent classification scheme for ternary fluid mixtures has been established, which is perhaps surprising in view of the importance of multicomponent mixtures for separation technology. Previous attempts at calculating phase diagrams of ternary fluid mixtures had mostly been made with the purpose of matching specific sets of experimental data, so that they cannot be regarded as systematic investigations of global phase behaviour; furthermore, some of the older work is incomplete in the sense that the global stability of the calculated critical states had not been checked.<sup>14–18</sup> In this work we present the first systematic approach to the global phase behaviour of ternary fluid mixtures.

## 2 Theory

### 2.1 Equation of state and mixing rules

As we are only interested in the topological properties of ternary mixtures, we use the van der Waals equation of state<sup>19</sup> for this investigation. From the literature on the global phase behaviour of binary mixtures it is known that—except for some “fingerprint domains”—all equations of state show a rather similar behaviour, hence the choice of the van der Waals equation simplifies the calculations without losing

generality:

$$p = \frac{RT}{V_m - b} - \frac{a}{V_m^2} \quad (1)$$

The substance-specific parameters  $a$  and  $b$  are related to the strength of the intermolecular attraction and the molecular size; they can be obtained from the critical data:

$$a = \frac{27}{64} \frac{R^2 T_c^2}{p_c} \quad b = \frac{1}{8} \frac{RT_c}{p_c} \quad (2)$$

This equation of state is extended towards mixtures by means of quadratic mixing and Lorentz–Berthelot combining rules:

$$\begin{aligned} a &= \sum_{i=1}^3 \sum_{k=1}^3 a_{ik} x_i x_k \\ b &= \sum_{i=1}^3 \sum_{k=1}^3 b_{ik} x_i x_k \\ a_{ik} &= (1 - \theta_{ik}) \sqrt{a_{ii} a_{kk}} \\ b_{ik} &= \frac{(1 - \eta_{ik})}{2} (b_{ii} + b_{kk}) \end{aligned} \quad (3)$$

Integration and addition of the mixing entropy term leads to the molar Helmholtz energy of a ternary mixture:

$$\begin{aligned} A_m(V_m, T, \vec{x}) &= \sum_{i=1}^3 x_i (\mu_i^\ominus + RT \ln x_i - RT) \\ &\quad - RT \ln \frac{V_m - b}{V_m^\ominus} - \frac{a}{V_m} \end{aligned} \quad (4)$$

$\mu_i^\ominus$  and  $V_m^\ominus = RT/p^\ominus$  denote the chemical potential of species  $i$  and its molar volume at a very low reference pressure  $p^\ominus$ , at which the perfect gas law applies.

### 2.2 Stability and critical states

The conditions for a critical point in a ternary mixture can be expressed as<sup>20</sup>

$$\begin{aligned} D^{(2)} &= \begin{vmatrix} G_{2x_1} & G_{x_1x_2} \\ G_{x_1x_2} & G_{2x_2} \end{vmatrix} = 0 \\ D^{(3)} &= \begin{vmatrix} G_{2x_1} & G_{x_1x_2} \\ D_{x_1}^{(2)} & D_{x_2}^{(2)} \end{vmatrix} = 0 \end{aligned} \quad (5)$$

where the shorthand notation  $G_{ix_1jx_2} = (\partial^{i+j} G_m / \partial x_1^i \partial x_2^j)_{p,T}$  has been used. A local stability criterion for a ternary critical

† Presented at the 1st Workshop on Global Phase Diagrams (Bunsen-Kolloquium 77), Walberberg, Germany, 21st–24th March 1999.

point is

$$D^{(4)} = \begin{vmatrix} G_{2x_1} & G_{x_1x_2} \\ D_{x_1}^{(3)} & D_{x_2}^{(3)} \end{vmatrix} > 0 \quad (6)$$

However, the Gibbs energy takes the pressure as a natural variable. In order to apply the conditions of criticality to pressure-explicit equations of state, which are functions of molar volume and temperature, it may be more convenient to express conditions (5) and (6) in terms of Helmholtz energies:

$$\begin{aligned} D^{(2)} &= \begin{vmatrix} A_{2V} & A_{Vx_1} & A_{Vx_2} \\ A_{Vx_1} & A_{2x_1} & A_{x_1x_2} \\ A_{Vx_2} & A_{x_1x_2} & A_{2x_2} \end{vmatrix} = 0 \\ D^{(3)} &= \begin{vmatrix} A_{2V} & A_{Vx_1} & A_{Vx_2} \\ A_{Vx_1} & A_{2x_1} & A_{x_1x_2} \\ D_V^{(2)} & D_{x_1}^{(2)} & D_{x_2}^{(2)} \end{vmatrix} = 0 \\ D^{(4)} &= \begin{vmatrix} A_{2V} & A_{Vx_1} & A_{Vx_2} \\ A_{Vx_1} & A_{2x_1} & A_{x_1x_2} \\ D_V^{(3)} & D_{x_1}^{(3)} & D_{x_2}^{(3)} \end{vmatrix} > 0 \end{aligned} \quad (7)$$

where again a shorthand notation has been used:

$$A_{iV^jx_1^kx_2} = \left( \frac{\partial^{i+j+k} A_m}{\partial V_m^i \partial x_1^j \partial x_2^k} \right)_T \quad (8)$$

Solving these equations cannot be achieved by standard root finding algorithms. Instead we used an extension of methods proposed earlier:<sup>1,21</sup> For the van der Waals equation, all derivatives of the Helmholtz energy [eqn. (4)] with respect to the molar volume or the mole fractions are *linear* functions of temperature. Hence the spinodal criterion  $D^{(2)} = 0$  turns out to be a 3rd order polynomial in temperature. Hence

(i) the critical temperature can be calculated for given values of  $V_m$ ,  $x_1$ , and  $x_2$  by application of Cardano's method;

(ii) with this temperature  $D^{(3)}$  can then be evaluated.

These two steps are repeated for different values of  $V_m$ ; a change of sign in  $D^{(3)}$  indicates that a ternary critical point has been passed, which can then be accurately determined by means of a *regula falsi* iteration.

For a ternary system there are two degrees of freedom in a critical state calculation, hence  $x_1$  and  $x_2$  can be treated as independent properties.

A positive value of  $D^{(4)}$  guarantees only the local stability of a critical point. Let  $x_{1c}$ ,  $x_{2c}$ ,  $T_c$ ,  $V_{mc}$ , and  $p_c = p(V_{mc}, T_c, x_{2c})$  denote the coordinates of a ternary critical point. Then, in order to ensure global stability, one has to show that the Gibbs energy surface of the mixture at the critical pressure and temperature,

$$G_m(p_c, T_c, x_1, x_2) = A_m(V_m, T_c, x_1, x_2) + p_c V_m \quad (9)$$

with

$$p(V_m, T_c, x_1, x_2) = p_c$$

is always above the tangent plane at the critical point. The latter is given by

$$G_m^{\text{tangent}} = \sum_{i=1}^3 x_i \mu_i(p_c, T_c, x_{1c}, x_{2c}) \quad (10)$$

where the chemical potentials  $\mu_i$  are obtained from eqn. (4) and evaluated at the critical state:

$$\begin{aligned} \mu_i &= RT \left( \ln x_i - \ln \frac{V_m - b}{V_m^\ominus} - \frac{2 \sum_k x_k b_{ik} - b}{V_m - b} \right) \\ &\quad - \frac{2 \sum_k x_k a_{ik} - a}{V_m} \end{aligned} \quad (11)$$

Both Gibbs energy functions, eqns. (9) and (10) require the calculation of the molar volume for given pressure values by Cardano's method. The comparison of  $G_m$  and  $G_m^{\text{tangent}}$  has to

be performed for a representative number of  $(x_1, x_2)$  combinations and is the most time-consuming step in the calculation of a ternary phase diagram.

### 3 Phase diagram classes of ternary mixtures

#### 3.1 Dimensionless parameter ratios

Even for the simple van der Waals equation 12 parameters  $a_{ik}$  and  $b_{ik}$  are required to characterize a ternary mixture. In order to reduce the degrees of freedom in our survey of ternary phase diagram classes we define dimensionless parameters, following the definitions given elsewhere:<sup>6</sup>

$$\begin{aligned} \xi_{ik} &= \frac{b_{kk} - b_{ii}}{b_{kk} + b_{ii}} = \frac{V_{mc,k} - V_{mc,i}}{V_{mc,k} + V_{mc,i}} \\ \zeta_{ik} &= \frac{d_{kk} - d_{ii}}{d_{kk} + d_{ii}} = \frac{p_{c,k} - p_{c,i}}{p_{c,k} + p_{c,i}} \\ \eta_{ik} &= \frac{b_{kk} - 2b_{ik} + b_{ii}}{b_{kk} + b_{ii}} \\ \lambda_{ik} &= \frac{d_{kk} - 2d_{ik} + d_{ii}}{d_{kk} + d_{ii}} \end{aligned} \quad (12)$$

The interaction density  $d_{ik}$  is defined for the van der Waals equation by:

$$d_{ii} = \frac{a_{ik}}{b_{ii} b_{kk}} \quad (13)$$

These parameter ratios are not independent; combination of the equations above yields:

$$\xi_{jk} = \frac{\xi_{ik} - \xi_{ij}}{1 - \xi_{ij} \xi_{ik}} \quad \zeta_{jk} = \frac{\zeta_{ik} - \zeta_{ij}}{1 - \zeta_{ij} \zeta_{ik}} \quad (14)$$

We furthermore assume Berthelot–Lorentz combining rules [all  $\eta_{ik} = \theta_{ik} = 0$  in eqn. (3)], which is a reasonable approximation for many nonpolar mixtures. With this simplification the definition of  $\lambda_{ik}$  can be transformed by a somewhat lengthy calculation into

$$\lambda_{jk} = 1 - \sqrt{1 - \zeta_{jk}^2} \quad (15)$$

It is thus possible to express all the parameters of one of the binary subsystems of a ternary mixture by those of the two others, and only  $\xi_{12}$ ,  $\xi_{13}$ ,  $\zeta_{12}$ , and  $\zeta_{13}$  remain as independent parameters.

#### 3.2 Ternary global phase diagrams

Fig. 1 shows the global phase diagram of a *binary* van der Waals mixture for equal sized molecules ( $\zeta = 0$ ,  $\eta = 0$ ). Each point of the diagram represents a phase diagram of a mixture with the parameters specified. The curves shown are

(i) tricritical curves, along which phase diagrams can be found where a three-phase line shrinks to zero length (*e.g.*, transition from class II to IV);

(ii) double critical endpoint curves, which mark the joining of two three-phase line segments (*e.g.*, transition from class IV to V);

(iii) azeotropic boundary curves, representing phase diagrams with an azeotrope at composition  $x = 0$  or  $x = 1$  (*e.g.*, transition from class I to I-A);

(iv) and curves representing phase diagrams with critical azeotropic endpoints (transition from III-A to III-HA).

A more detailed discussion of this and similar global phase diagrams and the phase diagram classes involved are given in other publications of this Workshop.

The Berthelot–Lorentz combining rule (15) is represented by a semicircle, which intersects the tricritical curves and simultaneously the double critical endpoint curves in the van Laar points at  $\zeta = \pm 0.5$ . These points mark the transition from binary phase diagram class II (=  $1^P$  in the modern

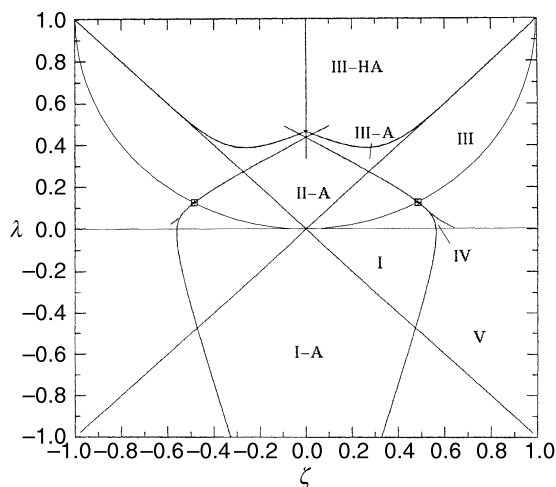


**Fig. 1** Global phase diagram of a binary mixture of equal-sized molecules (after Bolz). See text for explanation of curves.

nomenclature) to class III ( $= 1^c 1^z$ ). These two classes are the only ones possible under Berthelot–Lorentz combining rules.

The possible phase diagram class combinations for a ternary mixture are shown in Fig. 2, again for the case of equal-sized molecules. The horizontal and vertical boundaries mark the transitions II  $\rightarrow$  III or back for the 1–2 and the 1–3 subsystems; the curved boundaries represent the II  $\rightarrow$  III transition in the 2–3 subsystem [ $\zeta_{23} = 0.5$  in eqn. (14)].

The diagonal with the positive slope represents ternary mixtures with  $\zeta_{12} = \zeta_{13}$ , i.e. cases where the 1–2 subsystem and the 1–3 subsystem have become identical. The diagonal with the negative slope ( $\zeta_{12} = -\zeta_{13}$ ) represents ternary mixtures where the interaction parameter  $a_{33}$  is equal to the geometric mean of  $a_{11}$  and  $a_{22}$ .

Fig. 2 enables us to predict a ternary phase behaviour from the phase diagram classes of two of its binary subsystems.

For mixtures containing molecules of different sizes the Berthelot–Lorentz curve no longer passed through the van Laar point, but intersects the tricritical curves and the double critical endpoint curves at different  $\zeta$  values (see Fig. 1). Between these intersections domains of class IV ( $= 2^p l$ ) or IV\* ( $= 2^c 1^z$ ) can be found. The resulting global phase diagram is very similar to Fig. 2; the only difference is that the boundary lines become narrow bands of domains IV and IV\*. The rather complicated ternary phase diagram classes caused by the interaction of binary class IV with the other binary classes are not considered in this work.

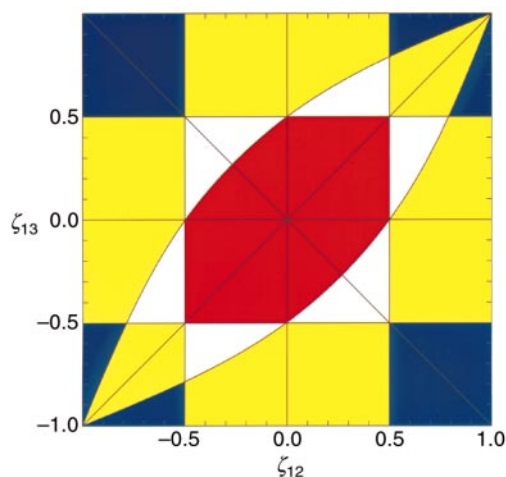


**Fig. 2** Global phase diagram of a ternary mixture of equal-sized molecules obeying the Berthelot–Lorentz combining rules. Field colours refer to the binary subsystems forming the ternary system: red: II + II + II, white: II + II + III, yellow: II + III + III, blue: III + III + III.

### 3.3 Ternary phase diagrams

From Fig. 2 one can conclude that there are 8 major ternary phase diagram classes. They are listed together with their constituting binary subsystems in Table 1.

Naturally, the two-dimensional representation of a four-dimensional ternary phase diagram ( $p, T, x_1, x_2$ ) is a rather difficult task. In this work we use two different graphical representations:

(i) a pseudobinary ( $p, T, x^*$ ) representation, where  $x^*$  denotes the relative amounts of the heavier components:  $x^* = x_2/(x_2 + x_3)$ . The sections at  $x^* = 0$  or  $x^* = 1$  represent true binary phase diagrams;

(ii) a prismatic pressure projection, where the vertical axis represents the critical pressure and the triangular prism base the ternary concentrations. It should be noted that in these diagrams the temperature is not constant along a critical plane.

The parameters of the equation of state which had been used to calculate the phase diagrams are given in Table 2 and in the figure captions. The (major) ternary phase diagram classes can then be described as follows:

*Ternary class I:* Phase diagrams of this class (Figs. 3 and 4) have closed  $lg$ -critical curves between the three critical points of the pure components. All binary subsystems are of the

**Table 1** Ternary phase diagram classes and classes of binary subsystems (assuming equal-sized molecules, Berthelot–Lorentz combining rules)

Binary subsystems			Ternary class
I	I	I	T-I
I	I	II	T-II
I	I	III	T-III
I	II	II	—
I	II	III	T-V
I	III	III	T-IV, T-V
II	II	II	T-VIII
II	II	III	—
II	III	III	—
III	III	III	T-VII

**Table 2** Van der Waals parameters used for the calculated ternary phase diagrams

$i$	$a_{ii}/$ bar dm <sup>6</sup> mol <sup>-2</sup>	$b_{ii}/$ cm <sup>3</sup> mol <sup>-1</sup>	$i$	$j$	$\theta_{ij}$	$\zeta_{ij}$
1	1.3572	32.1	1	2	0.00	0.00
2	2.3251	39.6	1	3	0.00	0.00

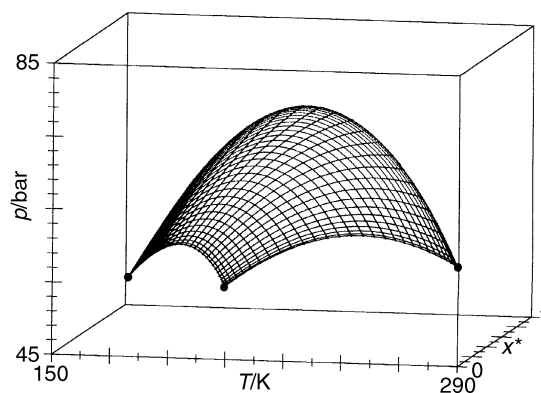


**Fig. 3** Critical surface of ternary class I—( $p, T, x^*$ ) representation. Circles: pure fluid critical points, dots: ternary critical points, parameters:  $a_{33} = 4.1697$  bar dm<sup>6</sup> mol<sup>-2</sup>,  $b_{33} = 0.0513$  dm<sup>3</sup> mol<sup>-1</sup> (other parameters listed in Table 2).

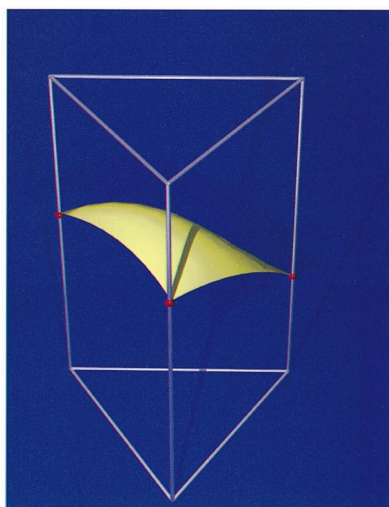


**Fig. 4** Ternary class I—prismatic representation (critical pressure *vs.* compositions—non-isothermal ( $p, x_1, x_2, x_3$ ) representation).

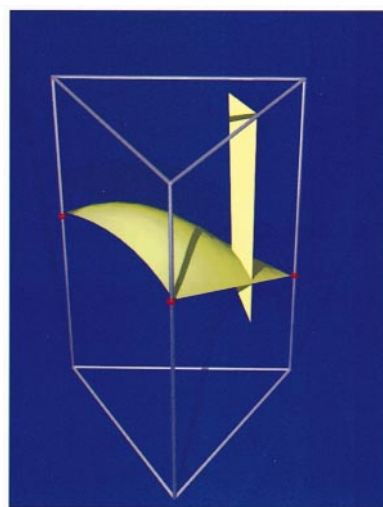


**Fig. 6** Ternary class II—prismatic representation.

binary type I according to the nomenclature of van Konynenburg and Scott.<sup>1</sup> This class is only possible for very similar chemical compounds.

**Ternary class II:** This ternary phase diagram has two binary subsystems of type I and one binary subsystem of type II. Consequently, there is—in addition to the *lg*-critical surface—an *ll*-critical plane at low temperatures (Figs. 5 and 6). Its border at low pressures, is a critical endpoint curve, which marks the beginning of a three-phase domain. This curve consists of upper critical endpoints and is called upper critical endline (UCEL) in this work.

**Ternary class III:** The ternary type III has one binary subsystem of type III and two binary subsystems of type I. There is only one contiguous critical plane, which appears to have a gash in it (Figs. 7 and 8). The rim of the gash is an UCEL, which ends in a tricritical point. Along the other side of the gash the critical plain runs to infinite pressures, and a continuous transition from *lg* to *ll* phase equilibria takes place.

**Ternary class IV:** This is one of the classes occurring if one binary subsystem is of type I and both other binary subsystems are of type III. Typical examples would be systems containing two similar heavy components plus one very light

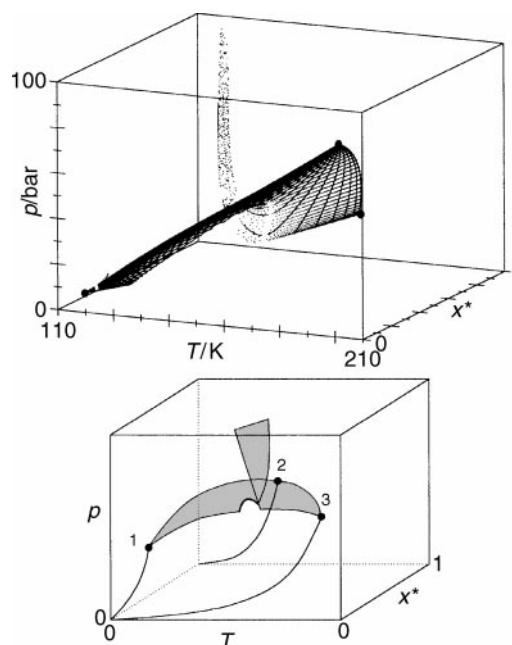


**Fig. 7** Ternary class III—( $p, T, x^*$ ) representation (calculated and schematic). Parameters:  $a_{33} = 4.1697 \text{ bar dm}^6 \text{ mol}^{-2}$ ,  $b_{33} = 0.1353 \text{ dm}^3 \text{ mol}^{-1}$ .

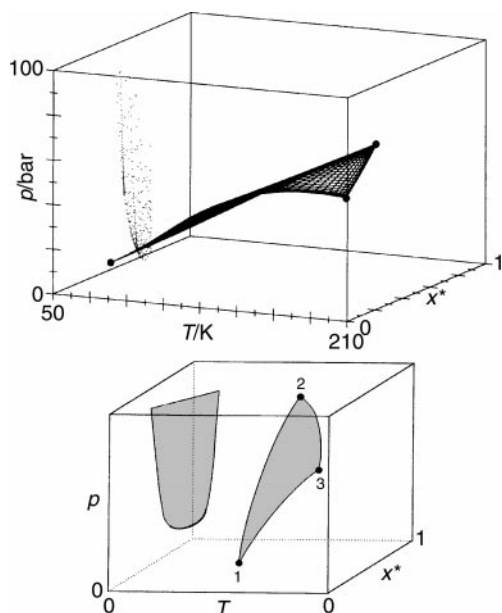


**Fig. 5** Ternary class II—( $p, T, x^*$ ) representation (calculated and schematic). Thin curves originating at  $T = 0$  are vapour-pressure curves. Parameters:  $a_{33} = 1.1697 \text{ bar dm}^6 \text{ mol}^{-2}$ ,  $b_{33} = 0.0513 \text{ dm}^3 \text{ mol}^{-1}$ .

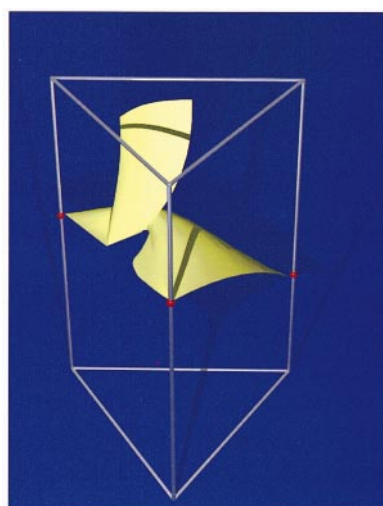


**Fig. 8** Ternary class III—prismatic representation.

component, which shows type III behaviour with either of the heavy ones. There is a large critical surface running upwards to infinite pressure at high temperatures, and a smaller one at low temperatures, which is bounded by an UCCEL (Figs. 9 and 10).

*Ternary class V:* Here the binary subsystems are of type I, II and III. This class is quite similar to class III, except that there is an additional *ll*-critical surface at low temperatures (Figs. 11 and 12).

*Ternary class VI:* This class is the “opposite” of ternary class IV. Again, the binary subsystems are of type I, III, and III, but now we have the case of two similar light compounds mixed with a heavy one. There are two critical surfaces; again the lower one is bounded by an UCCEL (Figs. 13 and 14).

*Ternary class VII:* All binary subsystems of the ternary type VII are of the binary type III. This ternary phase diagram has three critical planes. The critical surface of the component with the highest critical data shows *ll*-critical behaviour, the surface of the component with the lowest critical data *lg*-critical behaviour, and the third component has a critical plane showing *ll* critical behaviour with the light com-

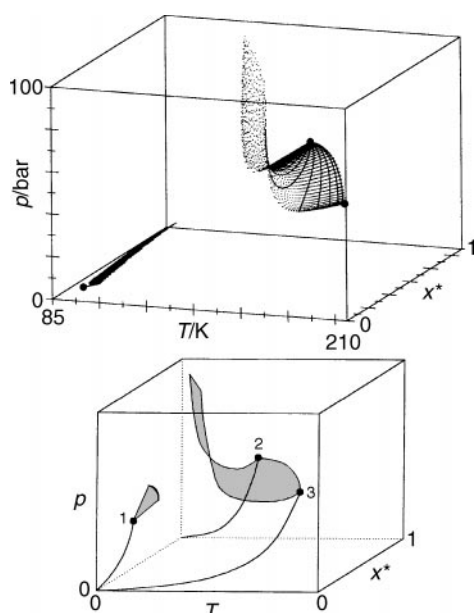


**Fig. 9** Ternary class IV—( $p$ ,  $T$ ,  $x^*$ ) representation (calculated and schematic). Parameters:  $a_{33} = 4.1697 \text{ bar dm}^6 \text{ mol}^{-2}$ ,  $b_{33} = 0.1513 \text{ dm}^3 \text{ mol}^{-1}$ .

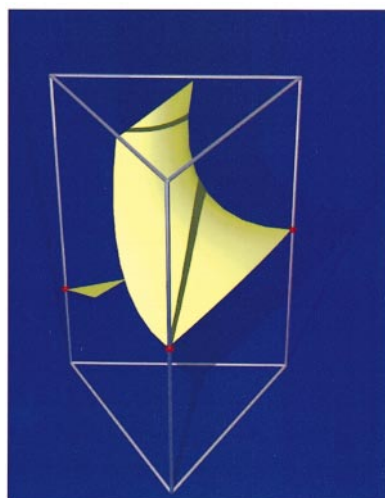


**Fig. 10** Ternary class IV—prismatic representation.

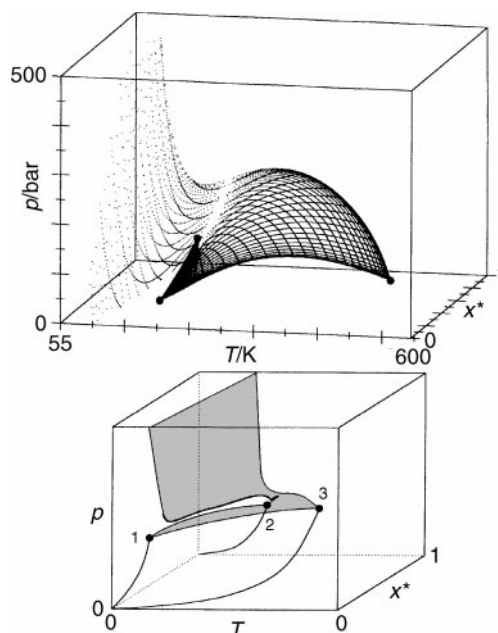


**Fig. 11** Ternary class V—( $p$ ,  $T$ ,  $x^*$ ) representation (calculated and schematic). Parameters:  $a_{33} = 8.1697 \text{ bar dm}^6 \text{ mol}^{-2}$ ,  $b_{33} = 0.0513 \text{ dm}^3 \text{ mol}^{-1}$ .

ponent and *lg* critical behaviour with the other one (Figs. 15 and 16).

*Ternary class VIII:* Finally there is a ternary class in which all binary subsystems are of type II. The phase diagram shows a contiguous *lg*-critical surface (as for the ternary class I), and in addition there are three *ll*-critical surfaces at lower temperatures (Fig. 17). Depending on the temperature ranges of the *ll* surfaces and binary interaction parameters of the mixture constituents several subtypes are conceivable; practically, however, these *ll* surfaces will probably be hidden by crystallisation.

It should be noted that several combinations of binary subsystem classes cannot occur under the conditions defined above. If some of the restrictions are dropped and molecules deviating from the Berthelot–Lorentz combining rules are considered, the number of possible ternary phase diagram classes becomes enormous. On the other hand, for practical purposes the number of distinguishable phase diagram classes may be smaller, because liquid–liquid immiscibility is often hidden by crystallization.

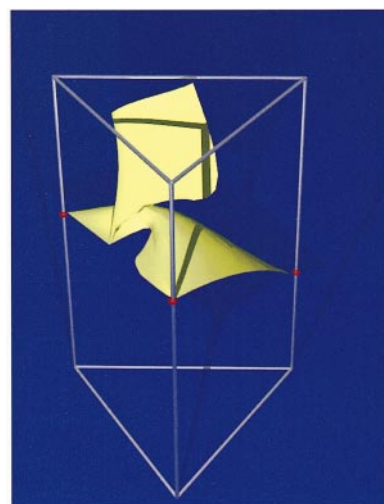


**Fig. 12** Ternary class V—prismatic representation.

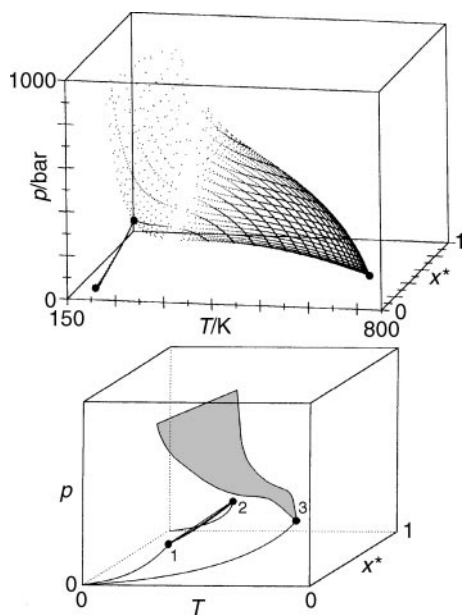


**Fig. 13** Ternary class VI—( $p$ ,  $T$ ,  $x^*$ ) representation (calculated and schematic). Parameters:  $a_{33} = 11.1697 \text{ bar dm}^6 \text{ mol}^{-2}$ ,  $b_{33} = 0.0513 \text{ dm}^3 \text{ mol}^{-1}$ .

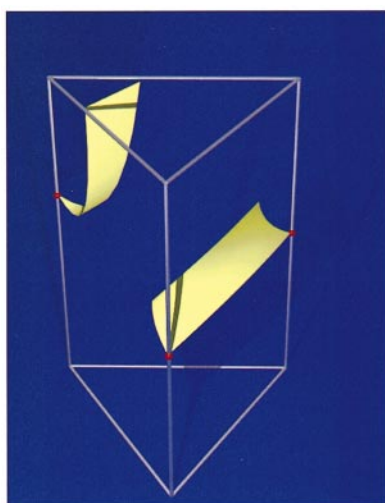


**Fig. 14** Ternary class VI—prismatic representation.

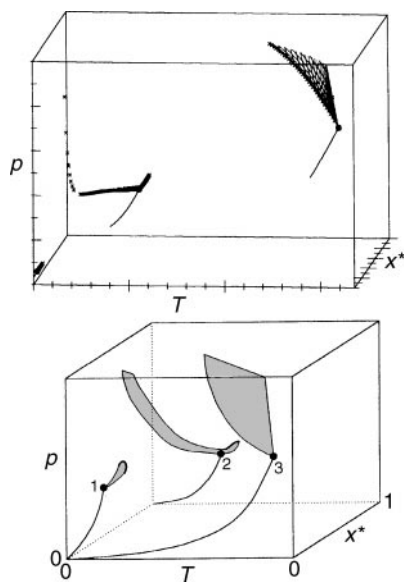


**Fig. 15** Ternary class VII—( $p$ ,  $T$ ,  $x^*$ ) representation (calculated and schematic).

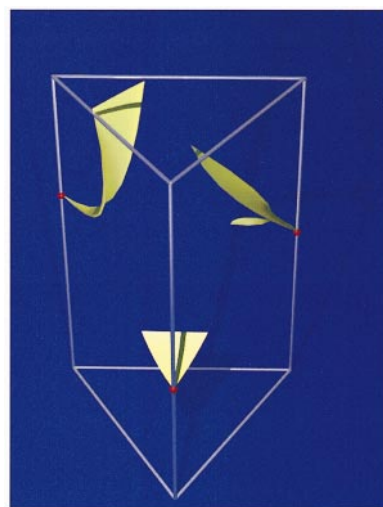


**Fig. 16** Ternary class VII—prismatic representation.

### 3.4 Miscibility windows

Ternary mixtures of ternary class IV can give rise to a peculiar phenomenon called *miscibility window*. If, due to cosolvency effects, a critical isopleth (at constant  $x^*$ ) is at lower pressure than its counterparts for the binary subsystems (at  $x^* = 0$  or  $x^* = 1$ ), an experimentalist would observe that a binary

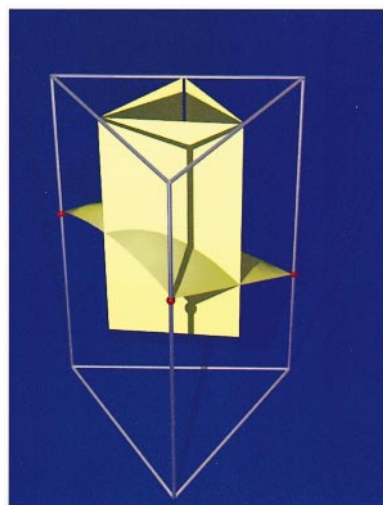


**Fig. 17** Ternary class VIII—prismatic representation.

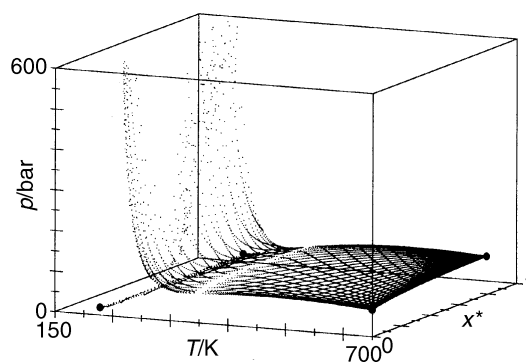


**Fig. 18** Ternary class IV with an isobaric miscibility window—( $p$ ,  $T$ ,  $x^*$ ) representation. Parameters:  $a_{11} = 20$ ,  $a_{22} = 23$ ,  $a_{33} = 8 \text{ bar dm}^6 \text{ mol}^{-2}$ ;  $b_{11} = b_{22} = 0.11$ ,  $b_{33} = 0.125 \text{ dm}^3 \text{ mol}^{-1}$ ;  $\theta_{12} = -0.08$ ,  $\zeta_{12} = -0.13$ ; all other  $\theta_{ij}$ ,  $\zeta_{ij}$  set to 0.

mixture in the two-phase state would become homogeneous and then heterogeneous again upon adding an amount of the third compound. The phenomenon can best be explained with the  $(p, T, x^*)$  phase diagram of ternary class IV: The high-temperature critical surface is formed like a chair; a depression in the “seat” gives rise to an isobaric miscibility window. An example is shown in Fig. 18. Likewise, a depression in the “back of the chair” would be noted as an isothermal miscibility window. The opposite effect, a diminished mutual miscibility of the ternary system, is called a *miscibility island*.

Both effects have been observed experimentally,<sup>22,23</sup> and have some significance for separation technology, e.g. for supercritical fluid extraction. It is interesting to note that even the van der Waals equation of state is able to reproduce these phenomena.

## 4 Conclusions

Even with the restriction to mixtures obeying the Berthelot–Lorentz combining rules, there is an impressive variety of ternary phase diagram classes, of which eight major classes have been outlined in this work. One of these classes, ternary class IV, is capable of producing the phenomena of miscibility windows even with the van der Waals equation of state. It is thus shown that miscibility windows are not necessarily caused by specific interactions between the mixture components, but are rather a topological phenomenon with no special requirements from the equation of state or mixing rules.

## 5 Acknowledgements

Financial support by the Deutsche Forschungsgemeinschaft as well as by the Fonds of the Chemical Industry is gratefully acknowledged.

## 6 Symbols

$A$	Helmholtz energy
$a$	attraction parameter of van der Waals equation
$b$	covolume parameter of van der Waals equation
$D^{(k)}$	stability determinant of $k$ th order
$G$	Gibbs energy
$n$	amount of substance
$p$	pressure
$R$	universal gas constant
$T$	temperature
$V$	volume
$x$	mole fraction
$x^*$	mole fraction of component 2 on a solvent-free basis
$\vec{x}$	vector of all mole fractions $x_i$
$\eta$	global phase diagram parameter: size nonadditivity
$\zeta$	global phase diagram parameter: pure component attraction parameter ratio
$\lambda$	global phase diagram parameter: binary attraction parameter ratio

$\mu$	chemical potential
$\xi$	global phase diagram parameter: pure component size ratio

### Subscripts:

$c$	critical property
$i$	referring to component $i$
$m$	molar property
$p$	derivative with respect to pressure (at constant temperature and composition)
$V$	derivative with respect to molar volume (at constant temperature and composition)
$x$	derivative with respect to mole fraction

### Superscripts:

$\ominus$	reference state
-----------	-----------------

## References

- 1 P. H. van Konynenburg and R. L. Scott, *Philos. Trans. R. Chem. Soc. London Ser. A*, 1980, **298**, 495.
- 2 L. Z. Boshkov, *Dokl. Akad. Nauk SSSR*, 1987, **294**, 901.
- 3 V. A. Mazur, L. Z. Boshkov and V. G. Murakhovsky, *Phys. Lett.*, 1984, **104A**, 415.
- 4 V. A. Mazur, L. Z. Boshkov and V. B. Fedorov, *Dokl. Akad. Nauk SSSR*, 1985, **282**, 137.
- 5 L. Z. Boshkov and V. A. Mazur, *Zh. Fiz. Khim. (Russ. J. Phys. Chem.)*, 1986, **60**, 29.
- 6 U. K. Deiters and I. L. Pegg, *J. Chem. Phys.*, 1989, **90**, 6632.
- 7 T. Kraska and U. K. Deiters, *J. Chem. Phys.*, 1992, **96**, 539.
- 8 A. Bolz, PhD Thesis, Ruhr-Universität Bochum, 1992.
- 9 A. van Pelt, C. J. Peters and J. de Swaan Arons, *J. Chem. Phys.*, 1991, **95**, 7569.
- 10 A. van Pelt and T. W. de Loos, *J. Chem. Phys.*, 1992, **97**, 1271.
- 11 J. Kolafa, I. Nezbeda, J. Pavlíček and W. R. Smith, *Fluid Phase Equilib.*, 1998, **146**, 103.
- 12 J. Kolafa, I. Nezbeda, J. Pavlíček and W. R. Smith, *Phys. Chem. Chem. Phys.*, 1999, **1**, 4233.
- 13 A. Bolz, U. K. Deiters, C. J. Peters and T. W. de Loos, *Pure Appl. Chem.*, 1998, **70**(11), 2233.
- 14 R. J. Sadus, *High Pressure Behaviour of Multicomponent Fluid Mixtures*, Elsevier, Amsterdam, 1992.
- 15 D. E. Mainwaring, R. J. Sadus and C. L. Young, *Fluid Phase Equilib.*, 1988, **42**, 85.
- 16 D. E. Mainwaring, R. J. Sadus and C. L. Young, *Chem. Eng. Sci.*, 1987, **42**, 1717.
- 17 M. Heilig and E. U. Franck, *Ber. Bunsen-Ges. Phys. Chem.*, 1989, **93**, 898.
- 18 M. Heilig and E. U. Franck, *Ber. Bunsen-Ges. Phys. Chem.*, 1990, **94**, 27.
- 19 J. D. van der Waals, *On the continuity of the gaseous and liquid states*, volume XIV of *Studies in Statistical Mechanics*, North-Holland, Amsterdam, 1988.
- 20 R. Haase, *Thermodynamik der Mischphasen*, Springer, Berlin, 1956.
- 21 U. Deiters and G. M. Schneider, *Ber. Bunsen-Ges. Phys. Chem.*, 1976, **80**, 1316.
- 22 M. Spee and G. M. Schneider, *Fluid Phase Equilib.*, 1991, **65**, 263.
- 23 A. Kordikowski and G. M. Schneider, *Fluid Phase Equilib.*, 1995, **105**, 129.

Paper 9/04863D